

## IN-SITU DIAGNOSTICS AT HIGH PRESSURES: ELLIPSOMETRIC AND RHEED STUDIES OF THE GROWTH OF $\text{YBa}_2\text{Cu}_3\text{O}_7$

DAVE H.A. BLANK, HORST ROGALLA

Low Temperature Division, Dept. of Applied Physics, University of Twente, Enschede, The Netherlands, d.h.a.blank@tn.utwente.nl

### ABSTRACT

Pulsed Laser and Sputter Deposition are used for the fabrication of complex oxide thin films at relatively high oxygen pressures (up to 0.5 mBar). This high pressure hampers the application of a number of *in-situ* diagnostic tools. One of the exceptions is ellipsometry. Using this technique we studied *in-situ* the growth of off-axis sputtered  $\text{YBa}_2\text{Cu}_3\text{O}_{6+x}$  thin films on (001)  $\text{SrTiO}_3$  as a function of the deposition parameters. Furthermore, the oxidation process from O(6) to O(7) has been studied by performing spectroscopic ellipsometry during isobaric cooling procedures.

Another suitable *in-situ* monitoring technique for the growth of thin films is Reflection High Energy Electron Diffraction (RHEED). In general this is a (high) vacuum technique. Here, we present an RHEED-system in which we can observe clear diffraction patterns up to a deposition pressure of 0.5 mBar. The system has been used for *in-situ* monitoring of the heteroepitaxial growth of  $\text{YBa}_2\text{Cu}_3\text{O}_{6+x}$  on  $\text{SrTiO}_3$  by pulsed laser deposition.

### INTRODUCTION

The relative high pressure during the deposition of, e.g., high Tc superconductors by (RF magnetron) sputter as well as pulsed laser deposition hampers *in-situ* diagnostics and monitoring of the growth. Reflection High Energy Electron Diffraction (RHEED) is a widely used technique for monitoring the growth of thin films in (high) vacuum. Several groups have monitored the growth of complex oxides with RHEED and have shown intensity oscillations, by depositing under pressures compatible with their RHEED set-up. To incorporate oxygen in the as-grown films, different alternatives were used, e.g., low pressures ( $10^{-6}$ - $10^{-4}$  mBar) of molecular oxygen,  $\text{NO}_2$ ,  $\text{O}_3$  or alternatively pulsed oxygen sources. In pulsed laser deposition (PLD), however, the background pressure during deposition is very important. It influences the oxidation process, the shape of the plasma plume and the growth parameters. Here, *in-situ* growth studies will be presented on  $\text{YBa}_2\text{Cu}_3\text{O}_{6+x}$  (YBCO) deposited by PLD at standard conditions, using a modified RHEED system.

Another monitoring technique, which can be used at higher pressures, is ellipsometry. It is non-destructive and can be used in any transparent medium. The major disadvantage of ellipsometry is the indirectness of the technique. The measured effective optical response can only be related to actual material properties by a model calculation. Nevertheless, real-time application of ellipsometry has proved to be a successful growth-analyzing instrument with sub-nanometer depth resolution. Moreover, studies have revealed that ellipsometry can be a sensitive oxygen content analyzing instrument by measuring the amplitude of the 4 eV optical excitation. Most ellipsometry studies are limited to measurements in *static* situations. Besides initial growth studies, we will present multi-wavelength dynamical oxygen loading measurements.

## ELLIPSOMETRY STUDIES ON YBCO

### Introduction

Ellipsometry is an optical surface analysis technique that exploits the change in polarization of light upon interaction with matter. The relative change of phase and amplitude of a linearly polarized light beam reflected on a surface material gives information about the properties of surfaces and interfaces. Usual applications of ellipsometry are determination of the thickness and the optical properties of thin films. The optical properties provide information about the composition and microstructure of materials. Furthermore it is possible to determine physical factors that affect these optical properties such as electric and magnetic fields, stress or temperature.

An important aspect of ellipsometry is that it is a non-destructive technique. As a consequence, it can be used for *in-situ* analysis which makes it possible to monitor thin-film or surface processes like deposition, oxidation, corrosion, adsorption, etching, diffusion etc. The only restriction is that the ambient in which the ellipsometric measurement takes place must be optically transparent. Several types of ellipsometers exist. The (reflection) ellipsometer used in this work is a so-called photometric (or intensity) ellipsometer. These instruments are based upon the variation of the detected light intensity consequent on the modulation of one or more optical parameters *e.g.* the polarizer or analyzer azimuth angle. In spectroscopic ellipsometry the dispersion in the complex index of refraction is measured.

Ellipsometry is a rather simple technique from a technically point of view but the interpretation of data can be very difficult because of the indirectness of the technique. As a consequence, representative optical models are necessary to relate the measured effective optical response of a material under investigation to its actual material properties. The necessity of model calculations is the largest drawback of ellipsometry, because the models are very complex in the case of multiple, inhomogeneous or rough films. Most of these models cannot be inverted analytically, with the consequence that material properties cannot be calculated directly from ellipsometric data (inverse problem). Other drawbacks are that the optical properties measured are a weighted average over the penetration depth of the light and the spot size and the technique is not element specific. Advantages are surface sensitivity, large energy resolution, sensitivity for the microstructure and the possibility to study the growth in a high background pressures.

### Experimental set-up

The experiments are performed with a spectroscopic P<sub>rot</sub>SA ellipsometer, which consists of an incoming optical bench (with a 75 W Xe discharge lamp and rotating polarizer) a deposition chamber and an outgoing optical bench (with analyzer and detector). Both polarizer and analyzer contain calcite Glan-Taylor prisms with an extinction ratio of  $10^{-7}$ . The polarizer (Bernard Halle element) and analyzer (Melles Griot element) have a beam deviation of 1' and 2.5', respectively. The detection system employs a multichannel analyzer consisting of a spectrograph and a 256-element linear photodiode array [1].

## Ellipsometric studies on YBCO

Using spectroscopic ellipsometry we studied *in-situ* the growth of off-axis sputtered YBCO thin films on (001) SrTiO<sub>3</sub> as a function of the deposition parameters. Especially in the very first growth stage (< 5nm) we observed that the optical properties of the grown layer differs from the 'bulk' optical properties of YBCO and strongly depend on, both, the deposition temperature and the oxygen partial pressure. Both properties are well established to influence the superconducting properties of thin YBCO films. In figure 1 the initial growth response of YBCO

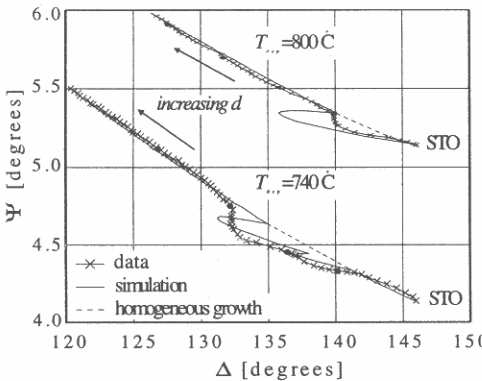


Figure 1:  $YBa_2Cu_3O_{6+x}$  initial growth response on STO at  $T_{dep}=800\text{ }^\circ\text{C}$  and  $T_{dep}=740\text{ }^\circ\text{C}$ ; The upper curve is shifted one degree upward for clarity. Black dots indicate 1 nm thickness increments. The photon energy is  $E=3.5\text{ eV}$ .

on STO at  $T_{dep}=800\text{ }^\circ\text{C}$  and  $T_{dep}=740\text{ }^\circ\text{C}$  are given. The upper curve is shifted one degree upward for clarity. Black dots indicate 1 nm thickness increments. The photon energy is  $E=3.5\text{ eV}$ .

The smoothness of the response is indicative for a step-mode like growth mechanism. The initial stage regime, however, is governed by a 2D-nucleation mechanism. This behaviour changes when the deposition temperature is lowered. Due to increased disorder, the initial stage regime is extended to larger thickness and a true-2D growth mode is no longer apparent. Similar behaviour is observed with increasing oxygen partial pressure, where the optical response is shifted from step-flow mode like mechanism to island-growth mode [2].

## Isothermic oxygen loading

The influence of the oxygen intake process on the  $YBa_2Cu_3O_{7-8}$  thin film pseudodielectric function is depicted in figure 2. The anneal temperature is kept constant at  $700\text{ }^\circ\text{C}$ . Subsequent spectra are taken after saturation of the optical response at the desired oxygen pressure. The saturation is reached typically within seconds and the rate of the oxygen indiffusion process seems to be only limited by the amount of oxygen flow needed to obtain higher background pressures. Two optical transition bands at 3.5 (CP1) and 4 eV (CP0) dominate the two panels of figure X. Both features decrease rapidly with increasing oxygen pressure, although the strength of CP1 does not change. The CP1 shows an energy shift towards the UV of 0.12 eV in the oxygen pressure range 0.1-10 mbar. The shift is 0.085 eV for CP0. With increasing oxygen pressure a small feature (CP2) at energy of 2.75 eV becomes visible.

## Isobaric oxygen loading

At the end of the isothermic oxygen anneal process upto a total pressure of 10 mbar, an isobaric cool down process step was performed. Results of this process are given in figure 3. In accordance with the CP0 behaviour with increasing oxygen pressure, a further decrease of the CP0 was observed until the excitation disappears at temperatures around  $550\text{ }^\circ\text{C}$ . The response of CP1 is somewhat different. The feature does not significantly decrease in strength, but shows a

strong energy shift towards the 4 eV band. The combined temperature effect on the two transitions results in an optical edge feature situated just below 3.9 eV at room temperature.

Interestingly, the amplitude of the CP2 in the imaginary part of  $\tilde{\epsilon}(E)$  first increases in strength with decreasing temperature, reaches a maximum at 550 °C and finally vanishes in the fully oxygenated state at room temperature. The overall resulting dielectric function at room temperature is in agreement, both in strength and energy behaviour, with literature results of  $\text{YBa}_2\text{Cu}_3\text{O}_7$  [3].

We attribute the amplitude behaviour of the CP0 and CP2 transitions around 550 °C to the tetragonal-orthorhombic phase transition. The assignment of the CP2 to Cu1-O1 transitions can also explain why the peak is not visible in the non-superconducting compound, where nearly no chain occupancy is present. Analogue peak behaviour was observed in literature at 4.8 eV [3], which is unfortunately out of our measurement range.

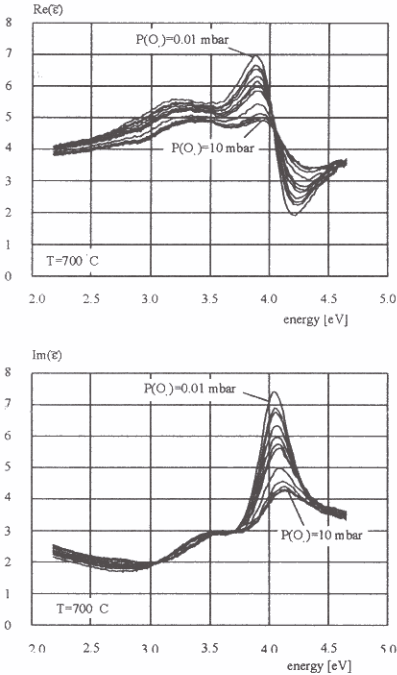


Figure 2: Oxygen loading dependence on pseudodielectric function of YBCO at  $T=700^\circ\text{C}$ . Oxygen pressures are: 0.01, 0.05, 0.1, 0.25, 0.5, 0.75, 1.0, 2.5, 5.0, 7.5 and 10 mbar, respectively.

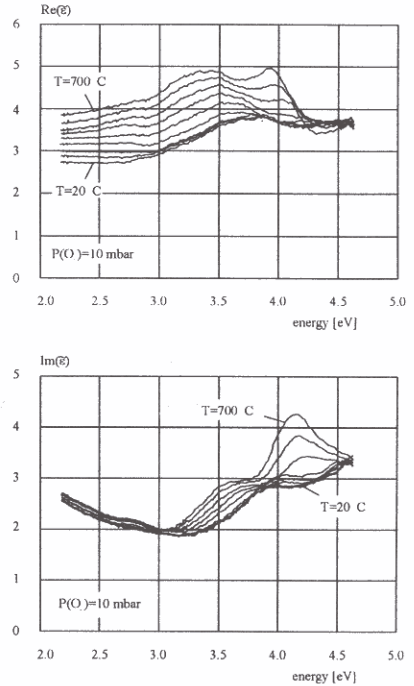


Figure 3: Isobaric oxygen loading of YBCO during cooling down. Oxygen pressure is 10 mbar. Temperatures are: 700, 650, 600, 550, 500, 450, 325, and  $20^\circ\text{C}$ , respectively.

## Real-time monitoring of isothermal oxygen indiffusion

In order to determine the chemical diffusion coefficient of the oxygen in YBCO thin films, a series of indiffusion experiments have been performed at different temperatures. By real-time monitoring of the dielectric function during oxygen loading an estimation of the diffusion coefficient  $D$  as a function of temperature can be made.

For each experiment the starting point in the phase diagram is  $pO_2=10^{-1}$  mbar at  $T=700$  °C, followed by a ramp down to a specific temperature for the diffusion experiment. When the temperature for the diffusion experiment is reached the real-time monitoring of the sample is started.

Figure 4 shows how the amplitude of the 4 eV transition decreases in time. The film thickness is determined as  $225\pm 15$  nm. Also indicated are the equilibrium values, as obtained by an isobaric cooldown in  $10^3$  mbar of oxygen. It can be seen that at a temperature of  $700$  °C, the time in which the amplitude of the 4 eV peak disappears after putting one bar of oxygen in the vacuum chamber, is in the same order of magnitude as the time resolution. At  $300$  °C there is still oxygen indiffusion but the process takes now several hours. At a temperature of  $200$  °C, within the error margins, no change in the peak is observed anymore.

It has also been observed that oxygen outdiffusion at  $600$  and  $700$  °C happens within the same time-scale as indiffusion. However, because it takes more than two minutes to pump down from 1 bar to  $10^{-1}$  mbar, accurate measurements were not possible.

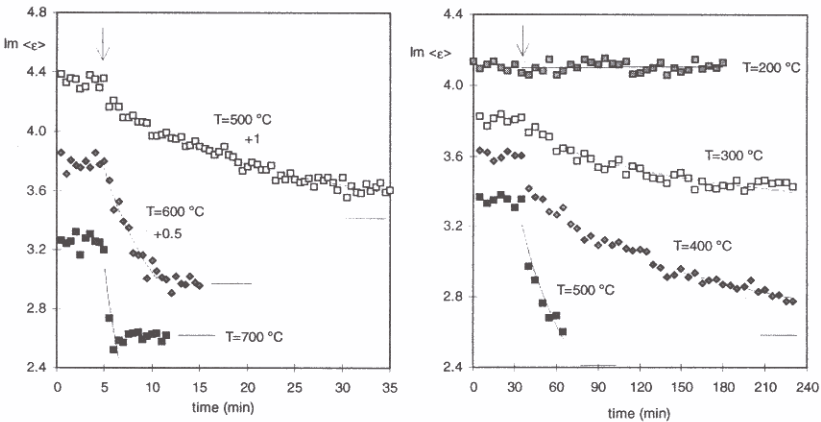


Figure 4: Change in the amplitude of the 4 eV transition during oxygen indiffusion at  $700$ ,  $600$  and  $500$  °C (a) and at  $400$ ,  $300$  and  $200$  °C (b). The arrow indicates the starting point and the lines are drawn to guide the eye. The  $600$  and  $500$  series are shifted upwards in (a) with  $0.5$  and  $1$ , respectively. Some points of the oxygen loading at  $500$  °C are plotted for comparison in (b). The stripes indicate the equilibrium values, obtained by an isobaric cooldown in  $10^3$  mbar  $O_2$ . The equilibrium values of the  $400$ ,  $300$  and  $200$  series are equal and indicated by the right stripe in (b).



# REFLECTION HIGH ENERGY ELECTRON DIFFRACTION

## Introduction

With RHEED an electron beam is directed to the substrate surface at a grazing angle. In this geometry the penetration depth is limited and, therefore, it is surface sensitive. A smooth and flat surface is represented by lattice rods in the reciprocal space. The rods are regularly spaced in an array with spacing of  $2\pi/a$  in the  $a^*$ -direction and  $2\pi/b$  in the  $b^*$ -direction. The intersection of the Ewald sphere leads to narrow streaks when a non-divergent monochromatic beam is used. Energy spread in the incident beam, detector resolution, non-elastic scattering and angular divergence of the beam cause the streaks to spread in the direction of the rods. The shape of the diffraction streaks gives information about the surface disorder. For example, a poor crystallinity can lead to fan-shaped streaks. Streaking is a phenomenon that is typical for RHEED, since the Ewald sphere and the reciprocal lattice rods are nearly parallel at low angle incidence, which means that a small degree of broadening of the rods can cause a large increase in the length of the diffraction condition. Lagally, Savage and Tringides [4] have written a comprehensive overview on RHEED from disordered surfaces, including a section on dynamical theory. They describe the consequences of certain surface disorders on the diffraction pattern.

The intensity of the diffraction spots varies during thin film growth, depending on the growth mode. Layer by layer growth, for instance, will lead to intensity oscillations. A maximum is reached after completing one monolayer. An increase of the surface roughness, e.g. island formation, will result in an overall decrease in RHEED intensity. Damping of the intensity oscillations reflects a mixture of layer by layer and island growth. Step propagation, or step-flow growth does not change the morphology of the substrate. The diffraction pattern and spot intensity will therefore stay constant during deposition.

Due to the grazing angle of the incident beam, surface roughness or asperities can produce a transmission diffraction pattern with sharp spots.

## Relaxations caused by pulsed deposition

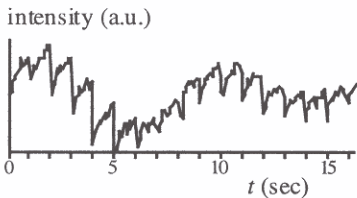


*Figure 5: Intensity oscillations of RHEED diffraction spot. Clearly visible are the relaxation caused by pulsed deposition*

During PLD every pulse produces a relatively large amount of material within several microseconds resulting in a high degree of disorder at the surface. The material will either nucleate on terraces or be adsorbed at step edges. This has a strong effect on the diffracted intensity, see figure 5. A sharp drop in intensity is followed by an exponential rise, characterised by a specific relaxation time constant. This constant depends on substrate temperature, surface condition, deposited material and the repetition rate of the laser pulse and, therefore, gives information about the mobility, diffusion velocity as well as diffusion lengths during deposition. This relaxation is seen superimposed on the RHEED oscillations.

## RHEED monitoring of YBCO

Since RHEED is a technique that is very suitable for the monitoring of the growth of thin films at high vacuum, this diffraction technique has been used during high vacuum growth of YBCO films. In 1990, Terashima *et al.* [5] were one of the first groups to report on RHEED

studies during YBCO growth on SrTiO<sub>3</sub>. The growth method they have applied was reactive evaporation, using a higher local oxygen pressure near the substrate (0.013 - 0.13 mbar) for oxygen incorporation, keeping the background pressure at  $1.3 \times 10^{-5}$  mbar. The intensity oscillations of the diffraction spots were related to the layer-by-layer growth of unit cell thick YBCO layers.

In 1993, Karl and Stritzker [6-8] reported on RHEED studies of YBCO film growth by PLD. To accomplish RHEED patterns at high enough pressures as possible for PLD of YBCO, a differentially pumped electron gun and integration of the intensity of the diffraction spots were used. Maintaining the pressure at the filament of the gun at  $10^{-6}$  mbar, they could reach an oxygen pressure of approximately  $10^{-2}$  mbar, which is still more than one order of magnitude lower than standard oxygen pressures during PLD of YBCO. They observed a relaxation of intensity after each laser pulse caused by the diffusion and nucleation on the surface immediately after the arrival of the material. They reported decreasing time constants with increasing temperature. Furthermore, they noticed the presence of a larger time constant due to the rearrangement of islands into fewer, larger islands – thereby decreasing the step density. This rearrangement and the related relaxation can be clearly seen after deposition. The intensity still increases slightly and more slowly, compared to the relaxation after each separate pulse.

Chern *et al.* [9] reported that RHEED oscillations could be restored after they had damped out, by interrupting growth for approximately 100 sec, keeping the sample at deposition temperature. This is a clear sign that thermodynamically, layer-by-layer growth is the preferred growth mode, but that limited kinetics is responsible for the development of Stranski-Krastanov growth.

More studies on pulsed laser deposition of YBCO have been reported, such as Russek *et al.* [10], who have done *ex-situ* RHEED after deposition of films ranging in thickness from 5 nm to 1  $\mu\text{m}$  on MgO, LaAlO<sub>3</sub> and NdGaO<sub>3</sub> substrates. One of the most interesting facets of their research has been the correlation between microscopic images and RHEED patterns.

Koinuma *et al.* [11] have reported on epitaxial growth of STO and YBCO on STO already in 1991. They applied PLD at low pressures and characterized the STO and YBCO films with several types of scanning probe microscopy [12].

The growth of SrCuO<sub>2</sub> on STO has been studied with *ex-situ* RHEED by Kawayama *et al.* [13]. The use of PLD to grow these films inhibited their use of RHEED during the growth. A large part of their work consisted of annealing studies of the STO substrate. They have found that high temperature annealing at 1 atm oxygen pressure delivered films with flat terraces and unit-cell steps.

Chandrasekhar *et al.* [14] and Terashima *et al.* [5] have reported the growth of YBCO films on STO with reactive coevaporation. They have observed an increase in intensity at the initial stage of the growth at the off-Bragg condition. This increase, however, is soon damped out. They also observed an increase in the oscillation time period after growth of several monolayers. Hirata *et al.* [15] have shown the nucleation of Cu islands at the initial stage of YBCO film growth on STO through study of the RHEED pattern changes during the growth of the first monolayer. After the formation of this initial copper oxide, the YBCO unit cells are stacked on top of them.

### RHEED at high pressures

All RHEED diagnostics presented above have one disadvantage: the low oxygen pressure. This (oxygen) background pressure, however, plays an important role in the deposition by PLD. First, oxygen reacts with the plasma particles, initiating the superconductive properties. Furthermore, the background pressure influences the shape of the plasma. The oxygen will slow

down the plasma, given its characteristic spheroid profile. But most of all, the relation between oxygen pressure and deposition temperature is important. If the pressure is too low, the temperature at which one can grow a stable structure has to be lower, reducing the crystallinity of the deposited film.

Rijnders *et al.* [16] developed a PLD-RHEED system which makes it possible to perform RHEED studies of PLD at standard deposition conditions. The most significant modification to the standard PLD system is the use of a two step differentially pumped electron gun, which secures the low pressure at the filament of the electron gun and a relative high pressure in the chamber (up to 0.5 mBar). The electron gun has been extended by a high vacuum tube that reaches 50 mm from the substrate while 50 mm further the diffraction pattern is projected onto a phosphor screen. A small aperture of 250  $\mu\text{m}$ , which limits the pressure leak from the chamber to the tube and the adjacent gun, restricts the connection between the tube and the chamber.

## EXPERIMENTAL RESULTS

### RHEED monitoring of YBCO

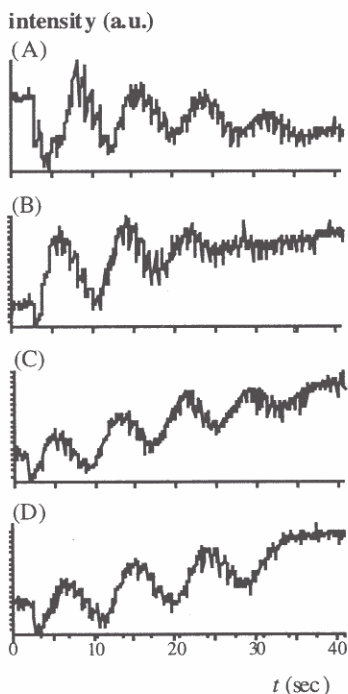


Figure 6: Intensity oscillations of YBCO during growth. A: starting deposition, B-D: after short anneal step at 850 °C.

Figure 6A shows a typical example of RHEED oscillations as observed during the growth of YBCO at standard PLD conditions. After completion of the first monolayer the intensity drops to 20 % of the initial intensity. Streaks replace the well-defined diffraction spots almost immediately. This behaviour is very typical for RHEED studies on YBCO, and is a natural response since formation of c-axis oriented YBCO unit-cells on an STO substrate inevitably leads to an increase in the number of steps on the surface. After four monolayers, the oscillations have almost vanished. The damping of the oscillations and its disappearance after four monolayers has frequently been reported. It is also common to see the decrease of intensity after the deposition of the first monolayer. This does not necessarily imply roughening, but could also be due to a decreased reflectivity of the deposited material relative to the substrate material. The appearance of streaks, however, is a clear indication for atomic roughening.

It is believed that the damping of the oscillations is caused by insufficient mobility of the YBCO unit-cells on the surface. Raising the deposition temperature can enhance the mobility, but this is limited due to the decomposition line of YBCO [17]. In general, with a background pressure of 0.15 mbar,  $\text{Cu}_2\text{O}$  outgrowths occur if the temperature exceeds 800°C. Growth interruption, allowing surface reconstruction, could be an alternative to smoothen the film. This effect can be observed by RHEED, by an increase of intensity after the deposition has been stopped.



Growth interruption usually has been applied at growth temperature, but mobility at these temperatures is slow. A higher temperature can increase the mobility.

In figure 6B-D the RHEED intensity during deposition of YBCO after an *in-situ* annealing (5 min. at 850 °C) is shown. Recovery of the RHEED oscillations during the growth of the first four monolayers of YBCO can clearly be seen, with a standard damping of the intensity oscillations. This is a direct consequence of the surface smoothing during the annealing step. The recovery of the oscillations can be repeated several times.

### Intensity relaxations

With PLD, it is possible to monitor the crystallisation of an amount of material that is deposited by looking at the relaxations of the intensity after each pulse. At pulse repetition rates of 1 Hz the initial nucleation will be dominant over the slower re-crystallisation and secondary diffusion mechanism. Karl and Stritzker [7] have done calculations on these relaxations at lower temperatures and pressure and showed that the diffusion constants are temperature dependent. The diffusion is reported to be faster at high temperatures, due to increasing mobility. They have assumed an exponential increase of intensity after each pulse, with which they associated a time constant  $\tau$ :

$$I = I_0 + A * (1 - e^{-(t-t_0)/\tau})$$

In this formula,  $I_0$  is the initial intensity immediately after the arrival of the adatoms at  $t_0$ , while  $A$  is the relaxation amplitude.

An exponential time constant is chosen, assuming an initial random distribution of material and nucleation sites. Random diffusion across the surface gives rise to an overall exponential time constant for the nucleation process. This time constant  $\tau$  depends on the density of

nucleation sites, the mobility and the diffusion velocity.

The relaxation times during growth of YBCO at different temperatures have been evaluated and it was found that the films grown at 760 °C have smaller time constants (ranging from 0.06 to 0.16 s) compared to films grown at 720 °C (ranging from 0.30 and 0.50 s). A lower diffusion velocity of the adatoms at lower temperatures can explain this. Increasing the temperature to 800 °C does not lead to shorter time constants (typical values found lie between 0.3 and 0.6 s).

This supports the idea that re-arrangements (or re-crystallization) are the dominant diffusion mechanisms at 800 °C.

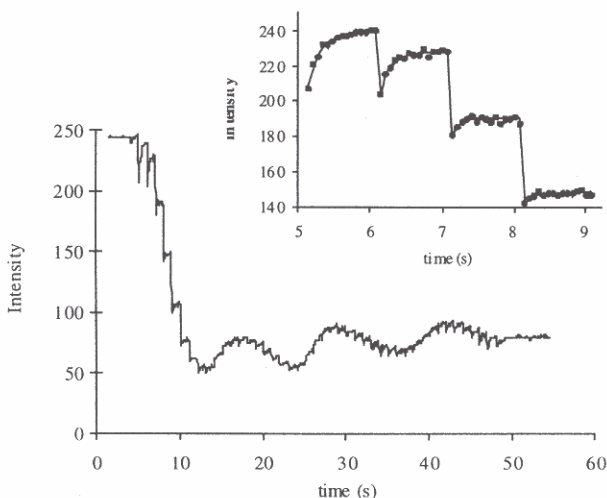


Figure 7: Intensity oscillations of the initial growth of YBCO. The inset shows the relaxations due to the pulsed laser

The time constants do not appear to be constant throughout the growth. Variations in the diffusion constants are expected because of the changes in step density during growth, as indicated by the intensity oscillations, see figure 7. The time constant  $\tau$  is expected to be smaller at a higher step density since these steps act as growth sites. Unfortunately, the relative change due to the relaxation becomes very small in a minimum of the intensity pattern. Therefore, it is very hard to calculate the time constant with enough accuracy. Nevertheless, with these first experiments an oscillatory behaviour of the time constants, similar to the RHEED intensity itself, can be distinguished.

Although these are primary results, and no hard conclusion can be made on these first experiments, it makes clear that applying RHEED at standard deposition pressures can lead to a better insight in thin film growth with PLD.

## CONCLUSIONS

Spectroscopic ellipsometry as well as Reflection High Energy Electron Diffraction are suitable analytical tools to study oxide materials made at relative high (oxygen) pressures. Although the latter technique has mostly been used under high vacuum conditions, a modification using a two step differentially pumped electron gun, makes it possible to apply RHEED up to 0.5 mBar background pressures.

With spectroscopic ellipsometry the phase diagram of YBCO has been studied by monitoring the optical response of *c*-axis oriented YBCO thin films during the initial growth, and isothermal and isobaric oxygen loading experiments. It is found that the 4 eV transition peak, which is associated with oxygen deficiency, vanishes before the YBCO is fully oxygenated. Besides, the transition strength is found to decrease more rapidly at higher temperatures as a function of the oxygen content. It is therefore argued that the 4 eV transition peak is sensitive to the oxygen ordering process in the Cu1 basal plane and might be a measure for the amount of tetragonal phase present in the YBCO film.

From real-time monitoring of the optical response during isothermal oxygen loading in the temperature range from 200 to 700 °C, the chemical diffusion coefficient *D* has been estimated and found to be  $\sim 10^{-12}$  cm<sup>2</sup>/s for 600-700 °C, and more than one order of magnitude smaller at 500 °C.

Although scattering of electrons in high oxygen pressure decreases the intensity of the electron beam, we have shown that growth monitoring of complex oxides at high oxygen pressures is feasible using RHEED. With this system we have monitored the growth of SrTiO<sub>3</sub> and YBCO using PLD at 0.15 mBar of oxygen. In both cases clear oscillations of the diffracted intensity are an evidence for two-dimensional growth, as expected from the crystal structure.

*In-situ* anneal steps between deposition steps improve the smoothness of the surface as indicated by the RHEED patterns. These results indicate the possibility of using the system for control of thin film growth on an atomic level even in quite high background pressures.

The relaxation times, due to the pulsed deposition, have been calculated for different deposition temperatures. It is found that films grown at 760 °C have smaller time constants (ranging from 0.06 to 0.16 s) compared to films grown at 720 °C (ranging from 0.30 and 0.50 s). Increasing the temperature to 800 °C does not lead to shorter time constants (typical values found lie between 0.3 and 0.6 s). First experiments show that the relaxation times depend on the step density during growth.

## ACKNOWLEDGMENTS

We gratefully acknowledge Marcel E. Bijlsma, Edward Span, Herbert Wormeester, for their work and discussions on the ellipsometric experiments and Guus J.H.M. Rijnders, Gertjan Koster, Joost Heutink and Boike L. Kropman for their work and discussions on the reflection high energy electron diffraction experiments. The analyses were performed in the Center of Materials Science (CMO) of the University of Twente.

This work is supported by the Dutch science foundation (FOM).

## REFERENCES:

1. Marcel E. Bijlsma, An *in-situ* ellipsometric study on high T<sub>c</sub> superconducting thin film growth, Thesis, University of Twente, ISBN 90-3650827-4 (1996).
2. M.E. Bijlsma, D.H.A. Blank, H. Wormeester, A. van Silfhout, H. Rogalla, J. Alloys and Comp., **251** (1997) pp. 15-18.
3. J. Kircher, M.K. Kelly, S. Rashkeev, M. Alouani, D. Fuchs and M. Cardona, Phys. Rev. **B44**, (1991), pp. 217.
4. M.G. Lagally, D.E. Savage, and M.C. Tringides, NATO ASI Series, Series B, Physics, **239**, cop. 1990, New York, Plenum Press in cooperation with NATO Scientific Affairs Division, pp. 139-174.
5. T.Terashima, Y Bando, K. Iijima, K. Yamamoto, K. Hirata, K. Hayashi, K. Kamigaki, and H. Terauchi, Phys. Rev. Lett. **65** (1990) pp. 2684-2687.
6. H. Karl and B. Stritzker, Phys. Rev. Lett. **69** (1992) pp. 2939-2942.
7. H. Karl and B. Stritzker, IEEE Trans. Appl. Supercond. **3** (1993) pp. 1594-1597.
8. H. Karl and B. Stritzker, Mat. Res. Soc. Symp. Proc. **285** (1993) pp. 269-274.
9. M.Y. Chern, A. Gupta, and B.W. Hussey, Appl. Phys. Lett. **60** (1992) pp. 3045-3047.
10. Stephen E. Russek, Alexana Roshko, Steven C. Sanders, David A. Rudman, J.W. Ekin, and John Moreland, Mat. Res. Soc. Symp. Proc. **285** (1993) pp. 305-310.
11. Hideomi Koinuma, Hirotohi Nagata, Tadashi Tsukahara, Satoshi Gonda, and Mamoru Yoshimoto, Appl. Phys. Lett. **58** (1991) pp. 2027-2029.
12. H. Koinuma, M. Yoshimoto, M. Kawasaki, H. Ohkubo, N. Kanda, and J.P. Gong, Mat. Res. Soc. Symp. Proc. **285** (1993) pp. 263-268.
13. I.Kawayama, M. Kanai, and T. Kawai, Jpn. J. Appl. Phys. **35** (1996) pp. 926-929.
14. N. Chandrasekhar, V.S. Achutharaman, V. Agrawal, and A.M. Goldman, Phys. Rev. B **46** (1992) pp. 8565-8572.
15. K. Hirata, F. Baudenraucher, and H. Kinder, Physica C **214** (1993) pp. 272-276.
16. Guus J.H.M. Rijnders, Gertjan Koster, Dave H.A. Blank, and Horst Rogalla, Appl. Phys. Lett. **70** (1997) pp. 1888-1890.
17. R.H. Hammond and R. Bormann, Physica C **162-164** (1989) pp. 703.